J. Membrane Biol. 167, 85–101 (1999)

The Journal of
Membrane
Biology

Endocytosis and Exocytosis Events Regulate Vesicle Traffic in Endothelial Cells

W.D. Niles*, A.B. Malik

Department of Pharmacology, University of Illinois College of Medicine, 835 South Wolcott Avenue (M/C 868), Chicago, IL 60612, USA

Abstract. We used water-soluble styryl pyridinium dyes that fluoresce at the membrane-water interface to study vesicle traffic in endothelial cells. Cultured endothelial cells derived from bovine and human pulmonary microvessels were incubated in styryl probes, washed to remove dye from the plasmalemmal outer face, and observed by digital fluorescence microscopy. Vesicles that derived from plasmalemma by endocytosis were filled with the styryl dye. These vesicles were distributed throughout the cytosol as numerous particles of heterogeneous diameter and brightness. Vesicle formation was activated 2-fold following addition of extracellular albumin whereas a control protein, immunoglobulin G, had no effect. Dye uptake was abrogated by labeling at low temperatures and inhibitors of phosphoinositide-3-kinase (PI 3-kinase). Tyrosine kinase inhibitors (genistein and herbimycin A) prevented the albumin-induced vesicle formation. Cytochalasin B prevented vesicle redistribution indicating involvement of actin filaments in translocation of endosomes away from sites of vesicle formation. Styryl dye was lost from cells by exocytosis as evident by the disappearance of discrete fluorescent particles. N-ethylmaleimide and *botulinum* toxin types A and B caused cells to accumulate increased number of vesicles suggesting that exocytosis was regulated by NSF-dependent SNARE mechanism. The results suggest that phosphoinositide metabolism regulates endocytosis in endothelial cells and that extracellular albumin activates endocytosis by a mechanism involving tyrosine phosphorylation, whereas exocytosis is a distinct process regulated by the SNARE machinery. The results support the hypothesis that albumin regulates its internalization and release in vascular endothelial cells via activation of specific endocytic and exocytic pathways.

Key words: Styryl pyridinium dyes — Digital fluorescence microscopy — Vesicle dynamics

Introduction

The microvascular endothelium is the primary barrier to exchange for macromolecules, liquid, and nutrients between the blood and tissue (Palade, 1953). Transport is mediated by two distinct pathways (Michel, 1992; Lum & Malik, 1994). Diffusive-convective flux through the paracellular pathway is controlled by endothelial cell contractility and integrity of interendothelial junctions (Renkin, 1985; Garcia et al., 1989). The transcellular pathway in endothelial cells utilizes vesicle trafficking (Palade, 1953) coupled to plasmalemma receptors for specific substrates such as albumin (Milici et al., 1987), transferrin (Jeffries et al., 1984), and insulin (King & Johnson, 1981). Because transcytosis enables receptor-mediated transport of substrates such as the osmotically active albumin molecule across the endothelial monolayer, the activation of endocytosis and exocytosis may be important in regulating tissue fluid homeostasis.

The mechanisms of endocytosis and exocytosis in endothelial cells are unclear. Fluid-phase and adsorptive markers placed in the capillary lumen adsorb to uncoated plasmalemma invaginations [i.e., the caveolae (Anderson, 1983; Parton, 1996)] and appear first in membrane-enclosed endosomes. These markers appear in ''omega-like'' caveolar invaginations of the albuminal plasmalemma and in the pericapillary interstitium on a time scale ranging from 5 sec to 20 min (Descamps, 1996; Ghitescu et al., 1986; Predescu et al., 1988). The cytosol of endothelial cells contains plasmalemma-derived vesicles (Hammersen, Hammersen & Osterkamp-Baust, 1983), variegated involutions of plasmalemma (Frøkjaer-

* *Present address:* Aurora Biosciences Corporation, 11010 Torreyana Road, San Diego, CA, USA

Correspondence to: A.B. Malik

Jensen, 1981), and fused vesicles and vacuoles (''vesicular-vacuolar organs'') connecting both luminal and albuminal plasmalemma (Dvorak et al., 1996). The significance of endothelial vesicles has been questioned because markers added to the capillary lumen such as cationic ferritin were not quantitatively represented in cytosolic vesicles (Clough, 1983).

Biochemical evidence indicates that endothelial cells have proteins required for endocytosis and exocytosis. Binding proteins for albumin (gp60) and tetrahydrofolate were localized in plasmalemma caveolae (Liu et al., 1986; Anderson, 1993; Tiruppathi et al., 1997). Microvascular endothelial cells have abundant caveolar plasmalemma invaginations (Schnitzer et al., 1994) and contain caveolin-1 (Tiruppathi et al., 1997). Internalization of plasmalemma caveolar proteins by vesicle formation requires hydrolysis of GTP (Schnitzer, Oh & McIntosh, 1996). Immunoreactive homologues of SNARE proteins that control exocytosis (Rothman, 1994) such as VAMP-2/synaptobrevin, SNAP, and N-ethylmaleimide (NEM)-Sensitive Fusion protein (NSF) also have been localized in endothelial caveolae (Schnitzer, Liu & Oh, 1995*b*). However, the role of SNARE proteins in exocytosis remains unclear because NEM inhibited transcytosis of albumin in capillaries (Predescu et al., 1994), whereas long exposures of cultured endothelial cells to NEM was shown to abolish endocytosis (Schnitzer, Allard & Oh, 1995*a*).

We used digital imaging fluorescence microscopy with styryl pyridinium dyes to study vesicle traffic in endothelial cells. Cultured endothelial cells are ideal for optical observation using these dyes because they are flat with thicknesses ranging from 200 to 800 nm. Styryl probes, used to study synaptic vesicle recycling at nerve terminals (Betz, Bewick & Ridge, 1993; Murthy & Stevens, 1998) and cell-cell fusion mediated by influenza hemagglutinin (Melikyan, White & Cohen, 1995), have physical properties that make them useful probes for study of vesicle traffic in endothelial cells. They fluoresce primarily at an interface between polar and nonpolar media while having a high solubility in water and low solubility in the hydrocarbon phase of membranes (Etaiw, Samy & Fayed, 1993). We exploited these properties to test the hypothesis that endothelial plasmalemma becomes incorporated into cytosolic vesicles and these vesicles are returned to the plasmalemma by exocytosis. We showed that the plasmalemma was constantly cycled in vesicles through the endothelial cell. Endocytosis was doubled in the presence of physiological concentrations of albumin, a response blocked by inhibitors of tyrosine kinases. Endocytosis was prevented by inhibitors of phosphoinositide metabolism and dye release was inhibited by blockers of SNARE machinery indicating that endocytosis and exocytosis in endothelial cells are regulated by distinct pathways.

Materials and Methods

Endothelial Cell Culture

Primary bovine pulmonary microvascular endothelial cells (BPMVEC) were cultured as described by us (Del Vecchio et al., 1992). Human pulmonary microvascular endothelial cells (HMVEC) and human pulmonary artery endothelial cells (HPAE) were obtained from Clonetics Laboratories (San Diego, CA). BPMVEC were grown in plastic flasks and maintained in high-glucose Dulbecco's modified Eagle's medium (DMEM, Gibco, Grand Island, NY) supplemented with 10% fetal bovine serum (FCS, Hyclone Laboratories, Logan, UT), 5 mM L-glutamine, 1 mM Eagle's nonessential amino acids, 50 U/ml penicillin, and 50 μg/ml streptomycin (Complete Growth Medium). HMVEC and HPAE were grown and maintained in Endothelial Growth Medium (EGM, Clonetics) supplemented with 10% FCS. Cells were passaged by standard technique at confluency (Del Vecchio et al., 1992; Folkman, Haudenschild & Zetter, 1979). Cells were grown and maintained in an incubator at 37°C in a 5% CO_2 atmosphere at 95% relative humidity, which also served as a controlled test chamber for dye labeling and other experimental manipulations.

For observation by microscopy, cells were grown on circular #1 glass coverslips coated with 0.1% gelatin. Coverslips were seeded with 5×10^4 cells, which was sufficient for complete coverage. The seeded cells were grown in 2 ml of Complete Growth Medium and used at >80% confluency (overnight to 2 days for BPMVEC and 5 to 7 days for HMVEC and HPAE). Confluent monolayers of endothelial cells were in all cases contact-inhibited (Folkman et al., 1979).

Fluorescent Dyes and Incubation Reagents

We used the styryl pyridinium probes N-(3-triethylaminopropyl)-4-(*p*-dibutylaminostyryl) pyridinium dibromide (FM 1-43) and N-(3-(triethylammonium) propyl)-4-(4-(*p*-diethylaminophenyl) butadienyl) pyridinium dibromide (RH 414) (Molecular Probes, Beaverton, OR). Stock solutions of 5 mg/ml dye in water were stored at −80°C for up to 1 month. Staining solutions were made by adding stock solution to Hanks Balanced Saline Solution (HBSS) containing 2 mM Ca^{2+} and 2 mM Mg^{2+} (divalent-HBSS). Rhodamine B dextran 20S (rho-dextran, Sigma Chemical, St. Louis, MO) was used to trace the fluid phase and the low-density lipoprotein (LDL) receptor substrate dil-LDL (Molecular Probes) was used to trace clathrin-coated pits. Both probes were suspended in divalent-HBSS immediately prior to use. Staining solutions and dye-free washing buffers usually contained bovine serum albumin (BSA-Fraction V, >99% purity, <1 ng endotoxin/mg, Sigma Chemical).

Cell Staining

Cultured cells on coverslips were labeled with styryl dyes by a standardized procedure. Growth medium was aspirated and cells were washed with 2 ml divalent-HBSS plus BSA at 37°C. After a brief wash with 1 ml of staining solution, cells were covered with 2 ml of fresh dye and incubated in a dark tissue culture incubator at 37°C unless otherwise indicated. At the end of staining, dye solution was decanted and cells were washed by rapid manual agitation with 3 changes of dye-free divalent-HBSS to remove all unincorporated styryl probe from the external surfaces of endothelial cells. Labeling with rho-dextran was performed by the same procedure; however, more extensive washing (>10 min) was required to remove the unincorporated rho-dextran.

For labeling with dil-LDL, a specific substrate for the LDL re-

ceptor in clathrin-coated pits on capillary endothelial cells (Pitas et al., 1985), cells were incubated in 10 μg/ml dil-LDL in HBSS at 37°C for 45 min. After 3 quick washes in dye-free HBSS at 37°C, dil-LDL associated with the external face of the plasmalemma was detached with 2 washes in ice-cold 100 mM NaCl, 50 mM Na acetate, pH 5.0, each 10-min duration (Dunn, McGraw & Maxfield, 1989). An ice-cold wash with pH 7.4 HBSS neutralized the pH.

Pharmacological Reagents

N-ethylmaleimide, cytochalasin B, *botulinum* toxin types A and B, Ly 294002, and rat IgG (Sigma Chemical) were stored dessicated at −80°C dilution in HBSS for immediate use. Wortmannin (Calbiochem, San Diego, CA), genistein, and herbimycin A (Calbiochem, San Diego, CA) were stored in dimethylsulfoxide at −20°C until dissolved in HBSS for use. Brefeldin A (LC Laboratories, Woburn, MA) was dissolved in water and then diluted in HBSS.

Chemical Fixation of Cells

For cell permeabilization studies, cells were fixed with 1% formaldehyde (Sigma Diagnostics, St. Louis, MO) in divalent-free HBSS without BSA at either 4 or 37°C. With cold fixation, the cells were initially cooled on ice for 15 min; this step was omitted with warm fixation. Cells were fixed in aldehyde solution either for 5 min at 37°C or for 30 min at 4°C. Fixed cells were washed for 30 min with 3 changes of HBSS, and residual aldehyde was quenched by incubation in 0.1 M glycine buffer for 15 min.

Fluorescence and Differential Interference Contrast (DIC) Microscopy

Stained cells were observed unfixed and live with an inverted microscope (Diaphot 200, Nikon, Garden City, NJ) equipped for both DIC and epifluorescence observation. For fluorescence observation, dye was excited by axially aligned, nonvergent Köhler illumination (Inoué, 1986) from a 100W Hg arc lamp operated with a stabilized power supply. Filters used to select excitation and emission wavelengths were the B-2A cube (Nikon) for FM 1-43 and the G-2E cube for RH 414, rho-dextran, and dil-LDL. Cells on coverslips were observed with a 60× oil-immersion objective (DIC 60 Plan Apo 1.4 N.A., Nikon). Transmission DIC observation was used to locate the focus plane for fluorescence observation and to evaluate the endothelial cell condition. Coverslips with any cells having vacuolated nuclear envelopes were discarded.

Image Acquisition and Processing

Fluorescence and DIC images were recorded for each cell field with a cooled, integrating CCD array camera (Imagepoint, Photometrics, Phoenix, AZ) connected to the microscope by a 0.6 × f/0.4 projection lens. Array integration times of 4 to 6 sec were necessary for the low-light level fluorescence images. The size of the readout frame was 750 vertical by 482 horizontal pixels and each pixel amplitude was digitized with a brightness resolution of 8 bits under computer control (Data-Stor P90, Data-Stor Marketing, Boulder, CO).

Quantitative analysis of images was performed with custom-written functions (Image Pro Plus Software Development Kit v. 1.3, Media Cybernetics, Silver Spring, MD; Visual C++ v. 1.6., Microsoft, Redmond, WA). Images were flat-field corrected, and paired DIC and fluorescence images were placed in registration using common landmarks. A background image, obtained from a cell-free field or by moving the focus plane below the specimen, was subtracted from each fluorescence image. Endothelial cell boundaries were located in the DIC image and overlaid on the paired fluorescence image to isolate cell fluorescence. Fluorescence brightness values, quantitated on a monochromatic scale of [0,255] units, were read for each pixel situated within the profile of each cell.

Linearity of the integrated CCD image (Aikens, Agard & Sedat, 1989) was determined with gelatinized coverslips bathed in 5 μg/ml FM 1-43. Intensity b was proportional to integration time t (100 msec to 20 sec) for brightness values ⩾230 units by the function $b = 4.214t - 0.429$ ($R^2 = 0.998$). This quantification ensured valid comparisons between brightnesses of different specimens.

Quantitation of Cell Fluorescence

Styryl dye fluorescence in cell images was quantitated by intensity distributions of identified particles (Russ, 1992). For pixels situated within the profiles of identified cells, spatial organization was determined by image segmentation into objects with the brightness range subdivided into 8 intervals. Each pixel was assigned to an intensity interval, and spatially connected pixels in the same interval were grouped into objects. Objects with areas <5.6 μm^2 (50 pixels) were subclassified as particles. Cell intensity was described by the distribution of the number of pixels in particles having brightness values of each of the 256 possible values. These particle brightness distributions were non-normal due to underdispersion. For example, distributions from 3 coverslips, seeded from the same batch of cells and labeled by the same procedure, failed the one-way analysis of variance test for homogeneity ($P < 0.01$, $F(3,1020) = 26,427$), although the differences were not significant in pairwise comparisons using the nonparametric 2-sample Kolmogorov-Smirnov test (all $P > 0.2$). Therefore, we used the medians and ranges of the particle brightness distributions to compare treatments; medians for replicated treatments were averaged. The proportion of cell image area covered by particles was calculated by summing the number of pixels in particles and dividing by the total number of pixels inside cell profiles. To calculate the fraction of cell brightness organized as particles, brightnesses of pixels in identified particles were summed and divided by the brightness sum for all pixels enclosed by cell profiles.

Measurement of Dye Loss From Stained Cells on Microscope Stage

To examine dye loss in microscopic detail, endothelial cells were maintained continuously on the microscope stage after labeling. The temperature at the object plane under epi-illumination was 29 ± 4°C. Labeled cells were washed with 37°C buffer and placed on the stage. Fluorescence loss was determined with a time series in which a fluorescence image was recorded once every 2 to 15 min with brief illumination for 4 to 6 sec to avoid dye bleaching. Fading was corrected with an internal reference in each field provided by either a dead cell or a large dye-filled vacuole. Continuous illumination caused the intensities of these reference spots to decrease at the same rate as vesicular particles. Reference intensities decreased by <0.5% during 1 hr (28-sec total illumination time); thus, the dye photodamage was minimized by this procedure.

To detect dye release immediately after labeling, cells still in dye-containing media were plunged into ice-cold buffer to arrest membrane dynamics. The cells were washed 3 times with cold buffer to remove external dye, and then rewarmed to 37°C. Within 15 min at

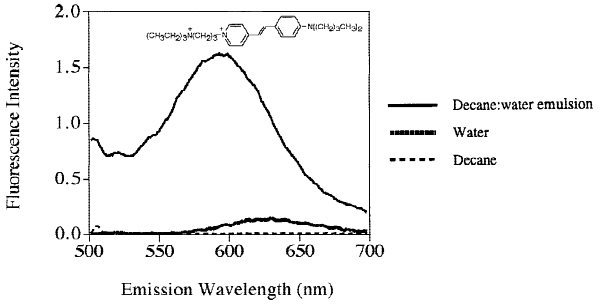

Fig. 1. Corrected fluorescence emission spectra of the styryl pyridinium dye FM 1-43 excited at 440 nm. FM 1-43 (5 μg/ml) in water (thick line), although readily soluble, was weakly fluorescent with a peak at 648 nm. Decane (dashed line) exposed to 5 mg/ml FM 1-43 showed no fluorescence, except for a very small peak at 505 nm. 5 μg/ml FM 1-43 in 1 ml water emulsified with 1 ml decane by 0.5% C12E9 (thin line) exhibited increased fluorescence and a blue-shifted polychromatic spectrum with a maximum at 593 nm. The requirement of a water-hydrocarbon interface for appreciable fluorescence and nonfluorescence in hydrocarbon indicated that the water-soluble FM 1-43 was useful for determining movements of plasmalemma-derived vesicles through endothelial cells. Inset: Molecular structure of FM 1-43.

37°C, the buffer was transferred to a fresh dish of unlabeled cells and plasmalemma fluorescence was examined.

Fluorescence Properties of Styryl Pyridinium Dyes

Our rationale for using styryl dyes was to unambiguously mark plasmalemma-derived vesicles. This interpretation hinged on 4 crucial physical properties: solubility in water with minimal fluorescence, insolubility (or nonfluorescence) in hydrocarbon, enhancement of fluorescence at a membrane-water interface, and rapid desorption from the interface. Because a systematic study of these properties has never been presented (Betz et al., 1992; Etaiw et al., 1993; Parda & Mishra, 1996), we examined the fluorescence properties of FM 1-43.

Fluorescence spectra were obtained with a spectrofluorimeter (SPF 500C, Aminco Bowman, Urbana, IL) with the photomultiplier tube operated at maximum dynode voltage and gain. The emission spectra shown in Fig. 1 were obtained with a 3-ml quartz cuvette containing 2 ml of 5 μg/ml FM 1-43. Dye was excited at 440 nm and fluorescence was read at 1 nm emission wavelength intervals with correlation for absorbance.

Although the dicationic FM 1-43 was readily soluble in water, its emission intensities were small as shown in Fig. 1 (thick line). FM 1-43 was insoluble and nonfluorescent in decane (dashed line). We tried 2 methods of solubilization, vortexing 3 ml of aqueous 50 μg/ml FM 1-43 with 3 ml of decane, and incubating a 5 &l aliquot of 5 mg/ml FM 1-43 in DMSO with 5 ml decane at 37°C for 24 hr. Neither method produced fluorescence in decane ($n = 5$) confirming that FM 1-43 is either insoluble in hydrocarbon and unable to partition into lipid bilayer membranes or nonfluorescent in aliphatic media. Emulsifying 5 μg/ml FM 1-43 in 1 ml water containing 0.5% C12E9 (CMC = 0.26%, Calbiochem, La Jolla, CA) in 1 ml decane, however, increased emission intensities by a factor >15 (thin line). The spectrum was polychromatic and blue-shifted consistent with stabilized π-orbital hybridization in the excited state by coplanarity of the anilinium and pyridinium rings at the water-hydrocarbon interface (Turro, 1978). At 520 nm, the ratio of emulsion-to-aqueous intensities was >35, indicating that the B-2A filter could discriminate between interfacial and aqueous probe. Emulsion breakage by excess water resulted in zero residual fluorescence in the decane. Neither detergent nor 10 mg/ml BSA increased intensities of FM 1-43 in water by >7%, indicating that the dye did not associate stably with either surfactant micelles or proteins. Because cell surfaces are complex, dye desorption was systematically studied using endothelial cells.

Results

Endocytosis of Plasmalemma by Endothelial Cells

Punctate Fluorescence in Endothelial Cells Stained with Styryl Dyes

Extracellular styryl dyes became incorporated into vesicles by cultured microvessel endothelial cells after incubation at 37°C for at least several minutes. The staining pattern obtained with FM 1-43 in Fig. 2*A* was typical. Fluorescence was due to the dye; autofluorescence by unstained cells was undetectable. Cell fluorescence was distributed throughout the cytosol except in dark areas corresponding to the nucleus as determined in the paired DIC image of Fig. 2*B.* The spatial distribution was punctate; bright discrete inclusions of dye with a broad distribution of diameters were resolved against a less bright and more diffuse but textured background. Particles had brightnesses ranging from 30 to 200 units that comprised ~50% of the total fluorescence intensity and occupied ~14% of the cell image area. The remaining fluorescence (intensity range from 10 to 50 units) was present in diffuse areas. Unwashed cells were uniformly bright due to dye adsorbed to external plasmalemma (Fig. 2*C*).

Fluorescent Particles Originate by Endocytosis

Punctate staining resulted from endocytosis during the period of dye incubation which enclosed styryl dye in cytosolic membrane-demarcated compartments. Endothelial cells equilibrated at 4°C before labeling did not retain fluorescence (Fig. 2*D*), although cells stained at 4°C and observed without washing were uniformly fluorescent as in Fig. 2*C*, indicating that cold abolished endocytosis without altering the dye fluorescence. Uptake was also abolished by pretreatment of endothelial cells at 37°C for 1 hr with 2 mM NaCN, NaN_3, or N-ethylmaleimide indicating that cellular metabolism was required for endocytosis. Since BSA was present in these experiments, punctate labeling also did not result from dye adsorption to nonpolar pockets of proteins on

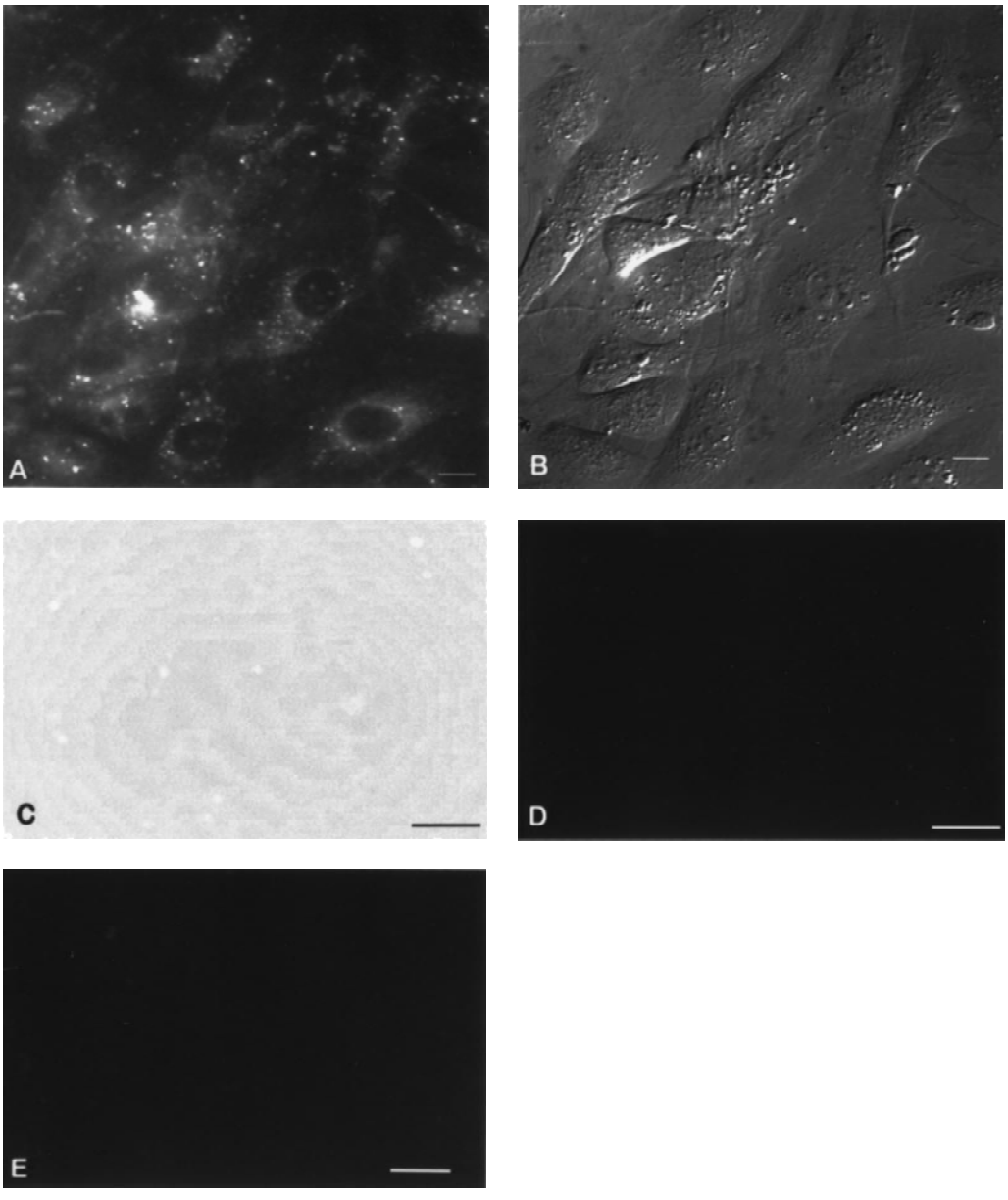

Fig. 2. Punctate fluorescence of BPMVEC stained with FM 1-43. BPMVEC grown to confluency on gelatin-coated glass coverslips were stained with 5 μg/ml FM 1-43 dissolved in HBSS plus 6 mg/ml BSA for 15 min at 37°C. Extracellular dye was removed by 3 rapid, brief washes in dye-free HBSS plus 6 mg/ml BSA at 37°C. (*A*) Cells observed through B-2A filter in epifluorescence. (*B*) Same field of cells in A observed in DIC optics. Dye is distributed in a punctate pattern throughout the cytosol. (*C*) Cells stained with FM 1-43 and examined without washing. Intense fluorescence originates from the dye adsorbed to external plasmalemma. (*D*) Cells cooled at 4°C for 30 min, stained at the same temperature with 5 μg/ml FM 1-43 for 15 min, and then washed with ice-cold buffer. Low temperature prevented particulate staining of endothelial cells with styryl dyes. (*E*) Endothelial cell membrane permeabilization by aldehyde. Cells were labeled with 5 μg/ml FM 1-43 for 15 min at 37°C, washed with dye-free buffer, and fixed in buffered 1% formaldehyde at 4°C for 30 min. Fixation permeabilized endothelial cell membranes enabling diffusion of the ~600 m.w. styryl probe from the cytosolic plasmalemma-derived vesicles. Results are typical of 5 experiments. All scale bars 10 μm.

the cell surface. Stained cells permeabilized with aldehyde completely lost fluorescence (Fig. 2*E*) because of leaching of dye during post-fixation washes. Exposing these fixed cells to styryl dyes resulted in uniform, non-punctate staining throughout ~10% of the cells.

Fluorescent Particles are not Connected to Plasmalemma

Punctate fluorescence originated from distinct vesicles within the cytosol. Regions of diminished, spatially un-

dulating brightness that were not optically resolved into particles (the diffuse regions) did not originate from styryl dye remaining adsorbed to plasmalemma after washing. When the extent and duration of the post-labeling washes were varied (Fig. 3*A–D*), one replacement of the labeling solution with dye-free buffer caused the greatest diminution of nonparticulate fluorescence (Fig. 3*A* and *E*). Further washing decreased background fluorescence and increased the number of resolvable particles per cell. After 3 washes, additional washing did not decrease the average brightness of the diffuse regions and, concomitantly, did not significantly increase the particle density (Fig. 3*C–E*), indicating that diffuse regions comprised clusters of plasmalemma-derived vesicles with subresolution diameters. In addition, extended washing did not diminish particle brightness (Fig. 3*E*). Thus, the staining pattern did not originate from dye trapped in long involutions of plasmalemma that would hinder removal of styryl dye from the external plasmalemma.

Concentration Dependence of Labeling Intensity and Kinetics of Endocytosis

Staining intensity depended on both styryl dye concentration and duration of labeling period. Concentration dependencies of labeling BPMVEC with FM 1-43 (black symbols) and RH 414 (white symbols) at 37°C are shown in Fig. 4*A*. Amount of dye incorporated in both particles and diffuse regions increased with dye concentration. RH 414 produced more intense staining than FM 1-43 (despite shorter incubation time) perhaps because of increased interfacial adsorption due to the extra olefin in its styryl linking group (Betz et al., 1992).

Kinetics of uptake were measured by varying the labeling duration. In Fig. 4*B*, cells were incubated at 37°C with either FM 1-43 (black) or RH 414 (white) for 2 to 60 min. Increasing duration of labeling increased both number of particles and intensities of diffuse regions. Staining intensity rapidly increased between 2 and 15 min and reached steady state between 15 and 45 min. Similar time- and concentration-dependencies were obtained with HPAE and HMVEC.

Styryl Dyes are More Effective than other Endocytosis Markers

Water-soluble interface probes were similar to traditional fluid-phase markers of endocytosis such as fluorescent dextrans but with 2 major exceptions. Highly fluorescent rhodamine B dextran 20S (rho-dextran) is widely used to detect endocytosis because its negative charge makes it water soluble and unable to associate with the anionic plasmalemma and glycocalyx. BPMVEC labeled with 200 μg/ml rho-dextran (equal in mole fraction to 5 μg/ml styryl dye) exhibited particulate staining but fewer vesicles were apparent and diffuse regions were less bright. Only the largest vesicles contained enough rho-dextran to form resolvable images, and smaller vesicles (comprising diffusely stained regions) contained few rho-dextran molecules.

Removal of external unincorporated rho-dextran was much more difficult than the styryl dyes. Punctate staining was present after 30 min washing in 2 out of 6 coverslips of cells cooled to 4°C for 1 hr to arrest endocytosis (Fig. 5*B*), whereas staining was completely absent from the other 4 coverslips. Thus, rho-dextran is a less reliable indicator of endocytosis than interfacial dyes. In addition, aldehyde-fixed cells could not be stained with rho-dextran ($n = 4$), indicating that permeation pathways created by aldehyde were too small for the 20,000 M.W. dextran.

BPMVEC stained with dil-LDL exhibited only ~1% of the number of particles as cells labeled with styryl dyes and these particles were much less bright (Fig. 5*C*). Since dil-LDL undergoes endocytosis triggered by specific receptors located in clathrin-coated pits on endothelial cells (Pitas et al., 1985), these data indicate that endocytosis by clathrin-coated pits in endothelial cells is small relative to uncoated pits.

Mechanisms of Endocytosis in Endothelial Cells

Stimulation of Styryl Dye Uptake by Extracellular Albumin

BPMVEC were incubated in serum-free HBSS for 12 hr and then in the test concentration of BSA for 4 hr prior to labeling. Endocytosis was unaffected with BSA concentrations ranging from 50 mg/ml to 10 μg/ml (Fig. 6). Uptake decreased by ~50% at 10 and 0.1 μg/ml BSA to values observed in the absence of serum albumin. Low albumin reduced endocytosis; i.e., number of particles was decreased and diffuse regions were less bright. This was not the result of decreased fluorescence of interfacial styryl pyridinium dyes because BSA had too small an effect on aqueous dye fluorescence to account for the 50% reduction in brightness secondary to deletion of BSA from the medium (*see* Materials and Methods). Albumin specifically stimulated the uptake since incubation of serum-depleted cells in rat IgG produced the same level of staining observed in the absence of albumin. Because plasma concentration of albumin ranges between 30 and 70 mg/ml and the K_d of albumin binding to endothelial cells is ~1 mg/ml, these results indicate that albumin-stimulated endocytosis operates at maximal rate over the psychological range of albumin concentration.

Tyrosine Kinase Inhibitors Prevent Albumin-induced Stimulation of Endocytosis

Incorporation of interface probes by endothelial cells maintained in BSA was decreased by ~50% in cells

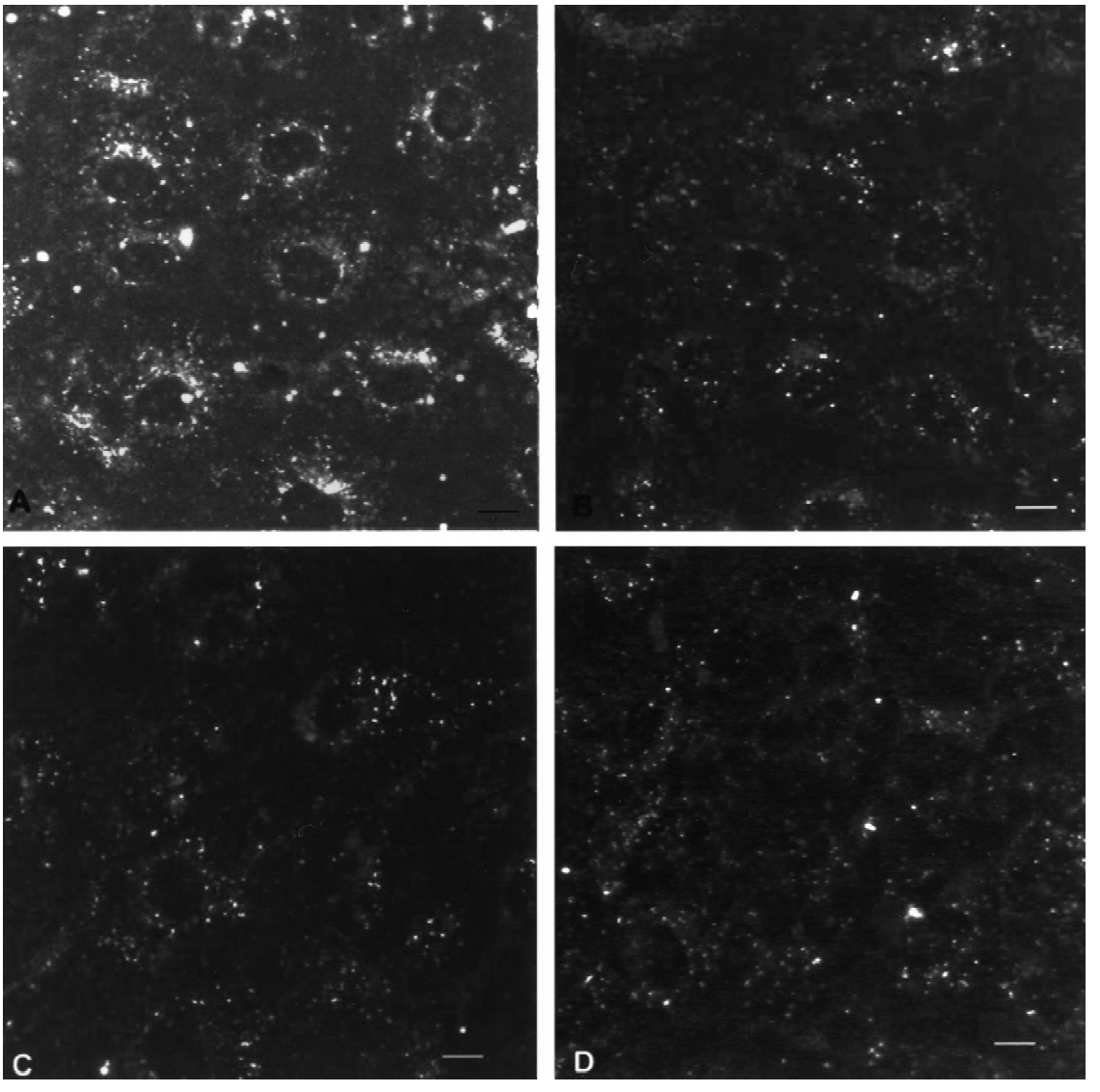

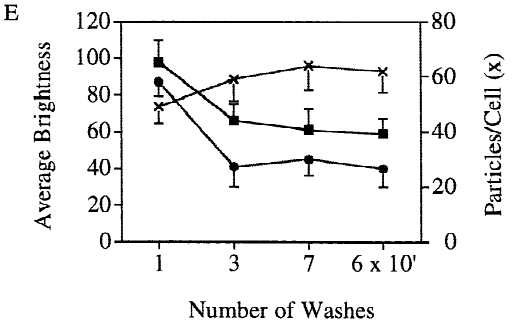

Fig. 3. Rapid desorption of external interfacial styryl dye from plasmalemma into dye-free buffer. BPMVEC were labeled by a 15-min incubation at 37°C in 5 μg/ml FM 1-43 in HBSS plus 6 mg/ml BSA. Coverslips were washed at 4°C. (*A*) The dye solution replaced once with 2 ml dye-free buffer. (*B*) Dye solution replaced with dye-free buffer, cells agitated for 2 sec, and the buffer replaced twice for a total of 3 washes. (*C*) Cells washed 7 times in dye-free buffer. (*D*) Cells were washed for 60 min with 6 changes of buffer. (*E*) Intensities of particles and diffusely stained regions. Particles were detected and classified by object recognition. Particle densities (crosses) were calculated by dividing the total number of particles by the total number of cells. Average particle brightness values (squares) were calculated by summing intensity values of all image pixels in particules and dividing by the number of pixels in particles. Average brightness values of diffuse cytosolic regions (circles) were determined from 8, 1 μm^2 areas selected in particle-free regions. These data show that particulate staining resulted from membrane-enclosed vesicles in the cytosol demarcated from the external medium. Data are representative of 4 experiments. All scale bars 10 μm.

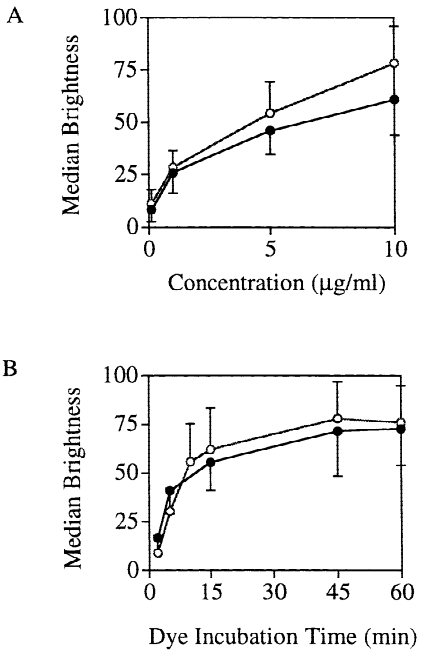

Fig. 4. Dependence of stained endothelial cell brightness on styryl dye concentration and duration of labeling period. (*A*) Concentration dependence. BPMVEC were labeled with FM 1-43 (black) for 15 min or RH 414 (white) for 10 min at 37°C and then washed with 3 rapid changes of dye-free buffer at 37°C. All buffers contained 6 mg/ml BSA. Three coverslips of cells were treated with each concentration. Medians of 3 distributions were averaged to generate each point. Error bar indicates range of medians around each average value. (*B*) Time dependence. BPMVEC were labeled with 5 μg/ml of either FM 1-43 (black symbols) or RH 414 (white symbols) and then washed. Medians and ranges of brightness distributions obtained at each point were determined as in *A*.

treated with 10 μM of either genistein (black) or herbimycin A (grey) compared to DMSO-treated controls (Fig. 7*A*). In serum-starved cells treated with genistein (hatched) or herbimycin A (white) in the absence of BSA, styryl dye uptake was not inhibited compared to serum-starved, BSA-depleted controls. These results show that only the BSA-stimulated component of endocytosis is sensitive to tyrosine kinase inhibitors. At tyrosine kinase inhibitor concentrations of 500 μM, however, dye incorporation was inhibited by >80% regardless of the medium BSA concentration, indicating nonspecific actions of these inhibitors. These data are consistent with the hypothesis that albumin activation of endocytosis relies on the tyrosine kinase pathway (Tiruppathi et al., 1997).

1-Phosphatidylinositol-3-Kinase Inhibitors Prevent Endocytosis

We found that endocytosis in endothelial cells was extremely sensitive at the early endosome stage of PI 3-kinase inhibitors, wortmannin and LY 294002. Endocytosis was decreased in endothelial cells incubated in wortmannin concentrations ranging from 20 mM to 1 μM with an EC_{50} of 20 nM (Fig. 7*B*) and dye uptake was abolished at concentrations >100 nM. LY 294002 was less effective, with an EC_{50} > 10 μM; 100 μM LY 294002 was required to inhibit endocytosis >80% (Fig. 7*B*). This effect of PI 3-kinase inhibitors was independent of extracellular albumin suggesting that they acted at the stage of plasmalemma vesicle budding rather than blocking either albumin-induced activation of endocytosis or post-endocytic processing (Joly, Kazlauskas & Corvera, 1995).

Cytochalasin B Blocks Translocation of Endosomes in Cytosol

The stereotypical pattern of endothelial cell labeling with styryl dyes was disturbed by the filamentous actin depolymerizing agent cytochalasin B. The morphology of endothelial cells treated with cytochalasin B was considerably altered (Fujimoto, Miyawaki & Mikoshiba, 1995) and dye was confined primarily to the cell periphery with a small amount diffusely distributed throughout the cytosol (Fig. 8*A*). Perinuclear staining was notably decreased compared to untreated cells (Fig. 8*B*). This surface fluorescence was impervious to extensive washing ($n = 4$), indicating enclosure of dye in vesicles adjacent to plasmalemma (this block was also seen with rhodextran). Thus, translocation of endosomes away from budding sites utilized an actin-based mechanism and the primary blockade of motility by cytochalasin B resulted in inhibition at the early endosome stage.

Endocytosis in Endothelial Cells is Unaffected by Brefeldin A

Brefeldin A treatment (up to 50 μg/ml for 1 hr prior to labeling) had no effect on uptake of styryl pyridinium dyes ($n = 8$). As Brefeldin A blocks membrane transfer through the Golgi apparatus by displacing guanine nucleotide from ADP-Ribosylation Factor-1 (Klausner, Donaldson & Lippincott-Schwartz, 1992), these results indicate that blockade of intracellular membrane pathways did not cause secondary block of plasmalemma internalization. Furthermore, Brefeldin A did not inhibit transcytosis of fluorescent BSA across cultured endothelium (Antohe et al., 1997), a finding consistent with our observation that a significant number of the plasmalemma-derived vesicles labeled by styryl pyridinium dyes are devoted to albumin-dependent endocytosis.

Fate of Plasmalemma-derived Vesicles in Endothelial Cells

Loss of Labeled Cell Fluorescence with Incubation

Styryl dye incorporated into endothelial cells by endocytosis was lost by several processes with different rates.

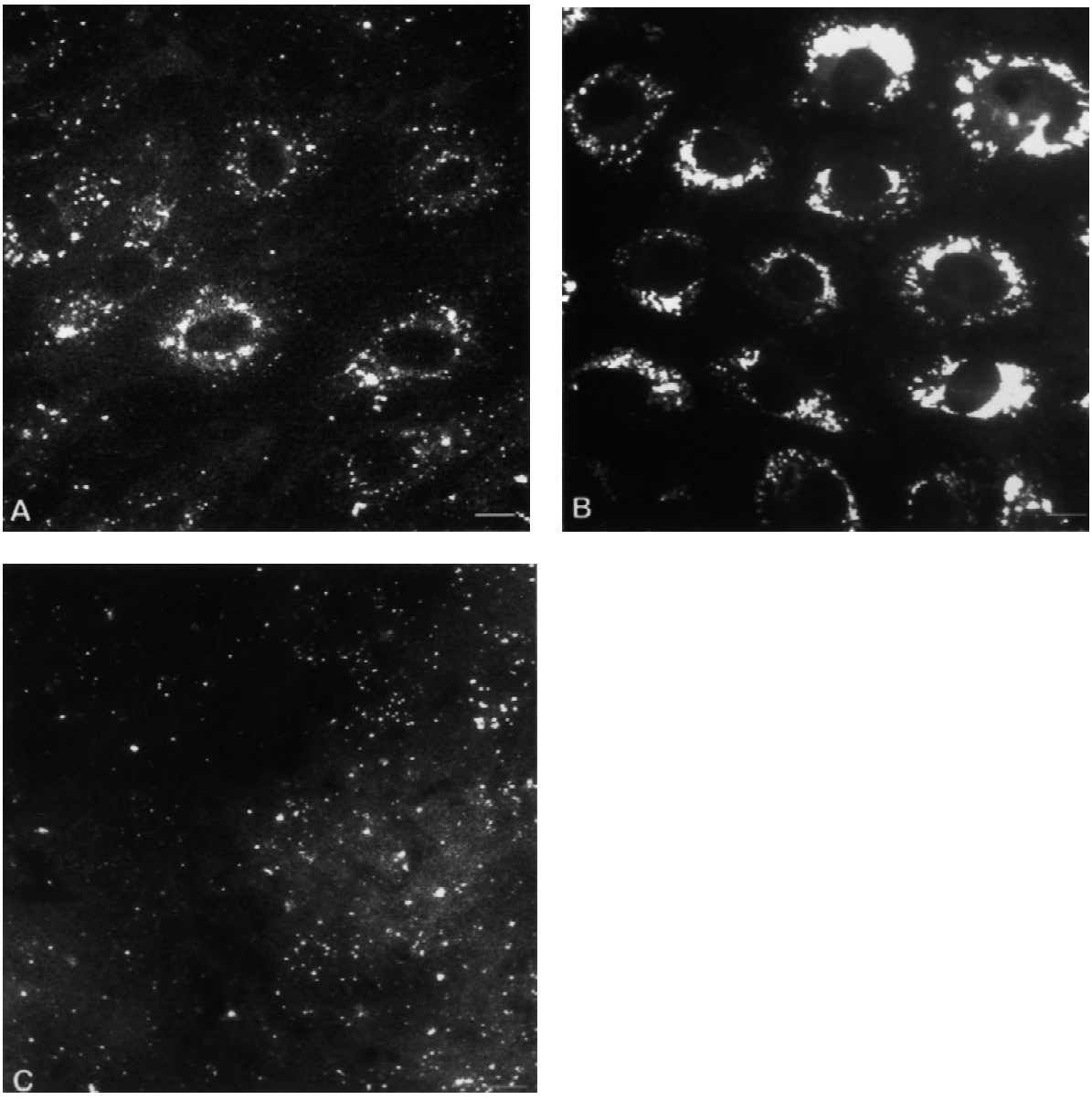

Fig. 5. Endothelial cell labeling by rhodamine B dextran 20S and dil-LDL. (*A*) Endocytosis of rho-dextran. BPMVEC were incubated with 200 μg/ml rho-dextran in HBSS plus 10 mg/ml BSA for 15 min at 37°C. Unincorporated dye was removed by 3 washes each 10 min in duration with dye-free buffer at 4°C. Staining with rho-dextran was low relative to the styryl dyes, because interfacial partitioning of the latter increases its concentration in endosomes. (*B)* Punctate staining with rho-dextran in the absence of endocytosis. BPMVEC, preincubated at 4°C for 1 hr were labeled and washed as in A but at 4°C. Particulate staining resulted from wash-resistant rho-dextran bound to discrete regions of plasmalemma. Staining at 4°C was never observed with styryl probes. (*C*) Endothelial cell labeling by dil-LDL. BPMVEC were labeled with 10 μg/ml dil-LDL In HBSS plus 10 mg/ml BSA for 45 min at 37°C. The cells were rinsed with dye-free ice-cold buffer and residual dil-LDL adhering to plasmalemma was removed with Na acetate pH 5.0 for 10 min. Few vesicles were labeled, indicating that a small area of plasmalemma mediates dil-LDL uptake via clathrin-coated pits in endothelial cells. In all panels, pixel intensities are multiplied by a factor of 3 for display. All scale bars 10 μm.

Immediately following labeling, cells began to liberate dye (*see* Materials and Methods), but the fluorescence was extremely low (<10 units) due to significant dilution into the wash medium and variable cell recovery kinetics from low temperatures. When multiple coverslips of cells seeded from the same culture were maintained in the dark and then periodically sampled, each batch lost styryl dye fluorescence with an exponential rate constant of $3.84 \pm 2.82 \times 10^{-2}$ hr^{-1} ($n = 9$). All cells lost >95% of their fluorescence by processes requiring cellular metabolism since maintenance at 4°C resulted in no loss of cell fluorescence. Because cells were confluent, their

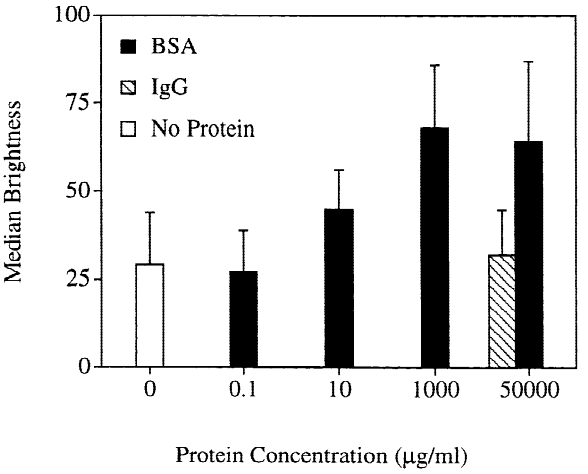

Fig. 6. Albumin concentration dependence of styryl dye uptake by endothelial cells. BPMVEC were depleted of albumin by incubation in divalent-HBSS for 12 hr at 37°C. Cells were then bathed in the indicated concentration of BSA for 4 hr at 37°C to replenish albumin in fiber matrix and at surfaces of cells. Cells were stained with 5 μg/ml FM 1-43 in the test BSA concentration for 15 min at 37°C and washed. Column heights show median brightnesses; bars indicate ranges of brightness distributions. Varying albumin from 50 mg/ml to 10 μg/ml slightly decreased styryl dye accumulation (black columns). At 100 ng/ml albumin, endocytosis was decreased by 50% to level of cells serum-depleted in HBSS containing no BSA for 16 hr and labeled in BSA-free dye (white column). Cells deprived of serum for 12 hr, equilibrated for 4 hr in 50 mg/ml rat IgG, and then labeled (grey column) incorporated the same amount of dye as cells labeled in albumin-free media, indicating albumin specificity. Half of membrane uptake in BPMVEC depends specifically on extracellular serum albumin.

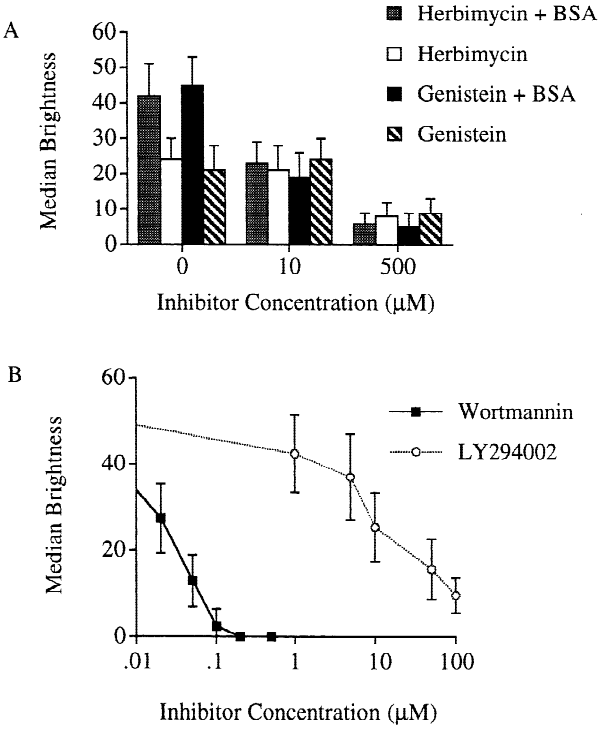

Fig. 7. Inhibitors of endothelial endocytosis. (*A*) Albumin-dependent inhibition by the tyrosine kinase inhibitors genistein and herbimycin A. BPMVEC were preincubated in divalent-HBSS at 37°C for 16 hr either in 10 mg/ml BSA or in protein-free buffer. During the final 30 min, cells were incubated in 10 μM or 500 μM of either genistein or herbimycin A (dissolved in 0.05% DMSO) or in HBSS containing only 0.05% DMSO. Inhibitor solutions contained BSA concentrations matched to those of the preincubations. Cells were stained with 5 μg/ml FM 1-43 in HBSS (with or without BSA as appropriate) for 15 min at 37°C and washed. Medians of brightness distributions for 3 coverslips subjected to the same treatment were averaged. Bars denote range of medians. DMSO-treated cells were randomly matched to the drug-treated cells. Tyrosine kinase inhibitors at 10 μM decreased endocytosis only when BSA was present, indicating inhibition of coupling between albumin binding and endocytosis. Column key: White-herbimycin A; Grey-herbimycin A plus BSA; Hatched-genistein; Black-genistein plus BSA. (*B*) Inhibition of endocytosis by 1-phosphatidylinositol-3-kinase inhibitors wortmannin (black) and LY 294002 (white). BPMVEC were incubated in albumin-free HBSS containing wortmannin or Ly 294002 for 30 min at 37°C. Cells were labeled with 5 μg/ml FM 1-43 for 15 min and washed. Control cells were incubated for 30 min at 37°C in 0.1% DMSO. Each point denotes the average median brightness for 3 experiments. Error bar denotes the median range.

long doubling times (Folkman et al., 1979) ruled out dye loss by dilution of vesicles into post-mitotic cells.

Disappearance of Discrete Fluorescent Particles

In time series images of stained cells maintained on the microscope stage after labeling (Materials and Methods), dye loss occurred by disappearance of discrete particles. To observe dye loss, we subtracted an image obtained at a later time from an earlier image obtained in a series of images of the same cells, as shown in an expanded image of a subcellular region (Fig. 9). Particles that moved rather than disappeared were identified by object tracking (Niles, Li & Cohen, 1992) and not scored as events. The difference image (Fig. 9*C*) shows that changes in fluorescence spatial distribution between early (Fig. 9*A*) and later images (Fig. 9*B*) occurred as discrete particles and portions of diffuse regions.

Particle disappearance events were random and not accompanied by changes in particle area or brightness. The average area (Fig. 9*D*) and brightness (Fig. 9*E*) of vesicles remained unchanged, and thus were not the result of fading or enzymatic degradation, which would cause smaller vesicles to disappear preferentially. Particle disappearance was also not secondary to fusion with lysosomes, which would cause the vesicles to increase in size and diminish in brightness. The dye content to each vesicle was instead lost in the ''all-or-none'' manner expected for exocytosis. Disappearances were uniformly distributed across all brightness classes of particles (Fig. 9*F*). Loss by the population of cells on each coverslip was well-fitted by an exponential rate equation with a rate constant of $0.131 \pm 0.053\ \text{min}^{-1}$ ($R^2 = 0.922$, $n =$

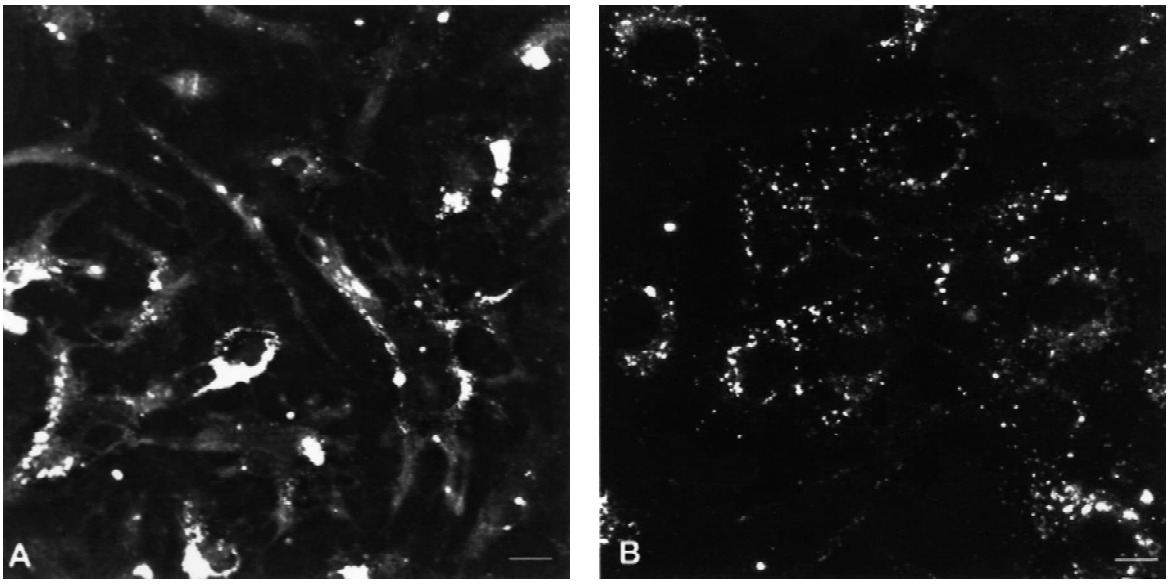

Fig. 8. Inhibition of vesicle translocation in cytosol after endocytosis by cytochalasin B. BPMVEC were incubated in 1 μg/ml cytochalasin B in HBSS plus 10 mg/ml BSA for 1 hr at 37°C, labeled with 5 μg/ml RH 414 for 10 min at 37°C, and washed for 15 min in dye-free buffer at 37°C. Cytochalasin B treatment altered pattern of cell labeling, vesicles were clustered near plasmalemma at the periphery of cells. Results indicate that translocation of plasmalemma-derived vesicles through cytosol after endocytosis is dependent on the actin cytoskeleton. (*A*) Cytochalasin-treated. (*B*) Untreated controls. Scale bars 10 μm.

16), revealing that a uniform first-order stochastic process governed particle disappearance. Particle disappearance rate was independent of image integration period and temporal separation between successive images in a series indicating that dye photobleaching was not the source of fluorescence decline. Particles were conserved between the early, later, and difference images (Fig. 9*F*) indicating that vesicular loss accounted for all fluorescence changes in cells maintained on the microscope stage. Disappearance of vesicles containing water-soluble fluorescent markers with the concomitant appearance of marker in a volume topologically equivalent to the vesicular interior is an indicator of membrane fusion (Niles & Cohen, 1987).

NEM Induces Accumulation of Vesicles

To assess occurrence of exocytosis and to probe regulation of membrane fusion in endothelial cells by N-ethylmaleimide-sensitive Fusion Factor (NSF) (Block et al., 1988), we incubated endothelial cells with NEM for <5 min prior to staining at 37°C. NEM increased the number of labeled vesicles (Fig. 10*A*, Fig. 11*B*) consistent with blockade of exocytosis. Treatments as short as 90 sec in 1 mM NEM were sufficient to enhance dye uptake (Fig. 10*A*). Pretreatment with 10 mM dithiothreitol for 30 min before and during treatment with NEM prevented the increase in styryl dye uptake. Incubation in 5 mM NEM for >5 min decreased dye uptake. NEM did not create independent permeation pathways for styryl dyes in the plasmalemma because cells treated with NEM at either 4 or 37°C and labeled in cold remained unstained. Labeling only at 37°C increased vesiculation indicating that NEM inhibited exocytosis.

Botulinum Toxins Increase Vesicle Number

We probed for function of Soluble NSF-Associated Protein (SNAP) Receptors (SNAREs), integral membrane proteins of vesicle (v-SNARES) and plasmalemma (t-SNARES) that are part of the exocytosis machinery (Rothman, 1994). SNAREs are cleaved by endopeptidase toxins from *Clostridium botulinum* (Block et al., 1988), which use sialic acid residues as endogenous receptors (Kozaki, 1979). Lectins densely bind to the external plasmalemma of caveolae in endothelial cells indicating extensive sialation of membrane constituents near sites of endocytosis and presence of *botulinum* toxin receptors (Simionescu & Simionescu, 1985, Predescu et al., 1988). Endothelial cells incubated with *botulinum* toxin type A (which targets t-SNAREs) or *botulinum* toxin type B (which targets v-SNAREs) accumulated in increased number of styryl dye-labeled vesicles relative to paired control cells (Fig. 10*B*, Fig. 11*C* and *D*). Increased dye uptake was not observed with inactivated NaOH-digested toxin. Increased uptake was unaffected by presence or absence of BSA in the incubation buffer indicating that *botulinum* toxins inhibited exocytosis of plasmalemma-derived vesicles of all origins.

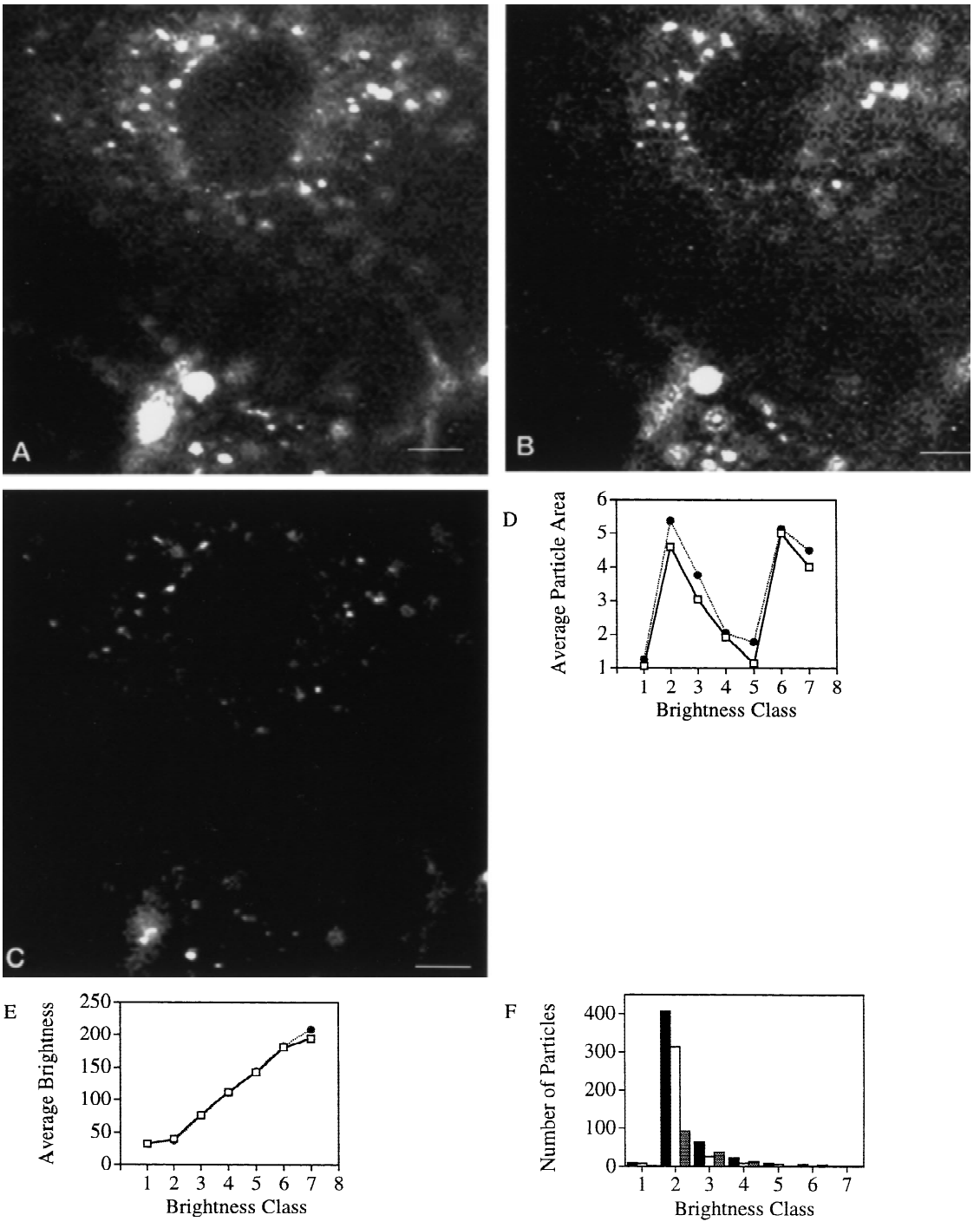

Fig. 9. Fluorescence decrease occurs by vesicle disappearance. Cells were labeled with RH 414 as in Fig. 8. (*A*) Fluorescence image of an area from a labeled cell 9 min after washing and placement on the microscope stage. (*B*) The same region after 30 min in the dark at a stage temperature of ~29°C. (*C*) Difference image of *A* − *B*. The difference image was comprised of discrete vesicles undergoing exocytosis between *A* and *B*. (*D*) Average areas of particles detected in full image frames from which A (black) and B (white) were obtained. The decrease in fluorescence between images A and B was not accompanied by significant changes in areas of particles in any brightness class (*see* Materials and Methods). (*E*) Average brightness values of particles detected in images A (black) and B (white). Fluorescent particles did not gradually dim, indicating expulsion of discrete vesicular contents of dye. Remaining styryl dye did not undergo fading or enzymatic degradation. (*F*) Histogram of particles in each brightness class in early (black), late (white), and difference (grey; i.e., the third bar of each brightness class) images. For each brightness class, the number of particles in the difference image equals the difference between numbers of particles in early and late images. This confirms conservation of particles and shows that loss of fluorescence occurred as exocytosis of discrete units of dye. Scale bars 5 μm.

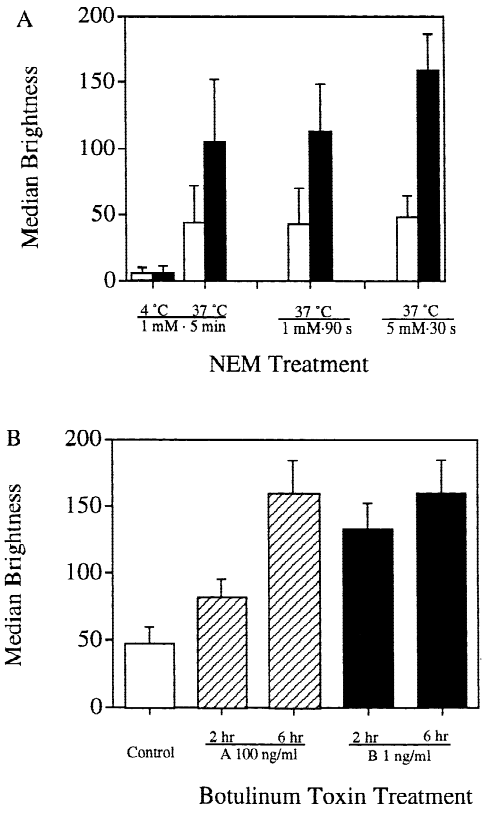

Fig. 10. Exocytosis inhibition increases dye uptake by endothelial cells. (*A*) N-ethylmaleimide (NEM) inhibits exocytosis in endothelial cells. BPMVEC were labeled by incubation in 5 μg/ml FM 1-43 for 5 min at either 37°C or 4°C (as indicated) and washed at the same temperature. Column height denotes averaged median brightness of 3 coverslips subjected to the same treatment. Error bars show maximum ranges of distributions. Left columns — BPMVEC cooled on ice to arrest endocytosis and incubated with 5 mM NEM for 5 min at 4°C prior to labeling. Paired controls were identically treated except for NEM. Second pair of columns — BPMVEC treated as above at 37°C. Increased labeling of NEM-treated cells at 37°C compared to 4°C indicated that endocytosis was required for styryl dye uptake. Two pairs of rightmost columns — NEM treatment for indicated time prior to labeling at 37°C reveals increase in dye uptake suggesting inhibition of exocytosis. Column key: White-control; Black-NEM-treated. (*B*) Exocytosis inhibition in endothelial cells by *Botulinum* toxin types A (hatched) and B (black). BPMVEC were incubated in toxin-containing HBSS plus 10 mg/ml BSA for the indicated duration. Control cells were incubated for the same duration in toxin-free HBSS plus 10 mg/ml BSA (white). All cells were labeled with 5 μg/ml RH 414 for 5 min at 37°C. Column height denotes averaged median brightness of 3 coverslips treated identically. Error bar depicts top range of medians. Toxin types A at 100 ng/ml and B at 1 ng/ml produced the same increased vesicle accumulation after 6 hr incubation in toxin, so this time was sufficient for toxin entry and action.

Discussion

Membrane Dynamics in Endothelial Cells Assessed by Styryl Pyridinium Dyes

Styryl pyridinium dyes combine advantages of fluid-phase and lipophilic membrane markers for probing membrane traffic in endothelial cells. Their water solubility enables easy removal of unincorporated plasmalemma dye and of dye subsequently released from cells by exocytosis. Because styryl dyes fluoresce predominantly at the interface between polar and nonpolar media, their enclosure by vesicles provided unambiguous assessment of vesicle formation (Fig. 1). Surface adsorption of styryl probes provides the fundamental advantage over fluid-phase markers. A lower concentration in the external medium is necessary to label the plasmalemma that then becomes internalized. Styryl dyes weakly adsorb to polar-nonpolar interfaces (ΔG ranges from −0.01 to +3.0 kcal/mol) (Parda & Mishra, 1996); thus, for a Boltzman distribution of molar fraction bound-to-free, $\exp(-\Delta G/RT)$, <½ of the molecules in the external solution are adsorbed to external plasmalemma face of endothelial cells. On a 25-mm coverslip covered with a confluent monolayer of cells bathed in 1 ml of 5 μg/ml styryl dye, ~1.6×10^{15} phospholipids (headgroup area of 0.6 nm^2) are exposed to an external solution containing 5 × 10^{15} dye molecules (this includes plasmalemma facing the gelatin-coated coverslip). Even if only 1% of dye partitions to membrane-water interface (3 dye molecules per 100 phospholipids), a 60 nm diameter endosome would contain >560 probe molecules. This value compared favorably with an equimolar concentration of the fluid-phase marker, rho-dextran. At 100 μg/ml rho-dextran in the external buffer, only 1 out of every 3 vesicles of the same size would contain ⩾1 rho-dextran molecules. The present observation that styryl dyes were more effective probes for detection of vesicles in endothelial cells than rho-dextran (Figs. 2 and 6) may be explained on this basis.

Vesicle Formation in Endothelial Cells

The mechanisms of formation of vesicles in endothelial cells remain controversial. Plasmalemma invaginations were seen in rapidly frozen and fixed endothelial cells from mesentery capillaries (Frøkjaer-Jensen, 1991), angiogenic capillaries of tumors, and endothelial cells exposed to Vascular Endothelial Growth Factor (VEGF) (Dvorak et al., 1996). In the present study, we showed that a remarkable feature of styryl dye uptake by endothelial cells is the particulate organization of fluorescence, which resulted from enclosure by vesicles of plasmalemma origin but not from entrapment in long invaginations of plasmalemma into the cytosol (Fig. 3). However, invaginations are noteworthy hallmarks of dynamic membrane (which would be captured by rapid freezing), as unpressurized phospholipid membrane vesicles undergo spontaneous curvature fluctuations and these coalesce into surface-connected tubules that relax by vesiculating (Döbereiner et al., 1993). Thus, vesicle budding may be driven by thermal fluctuations in lipid

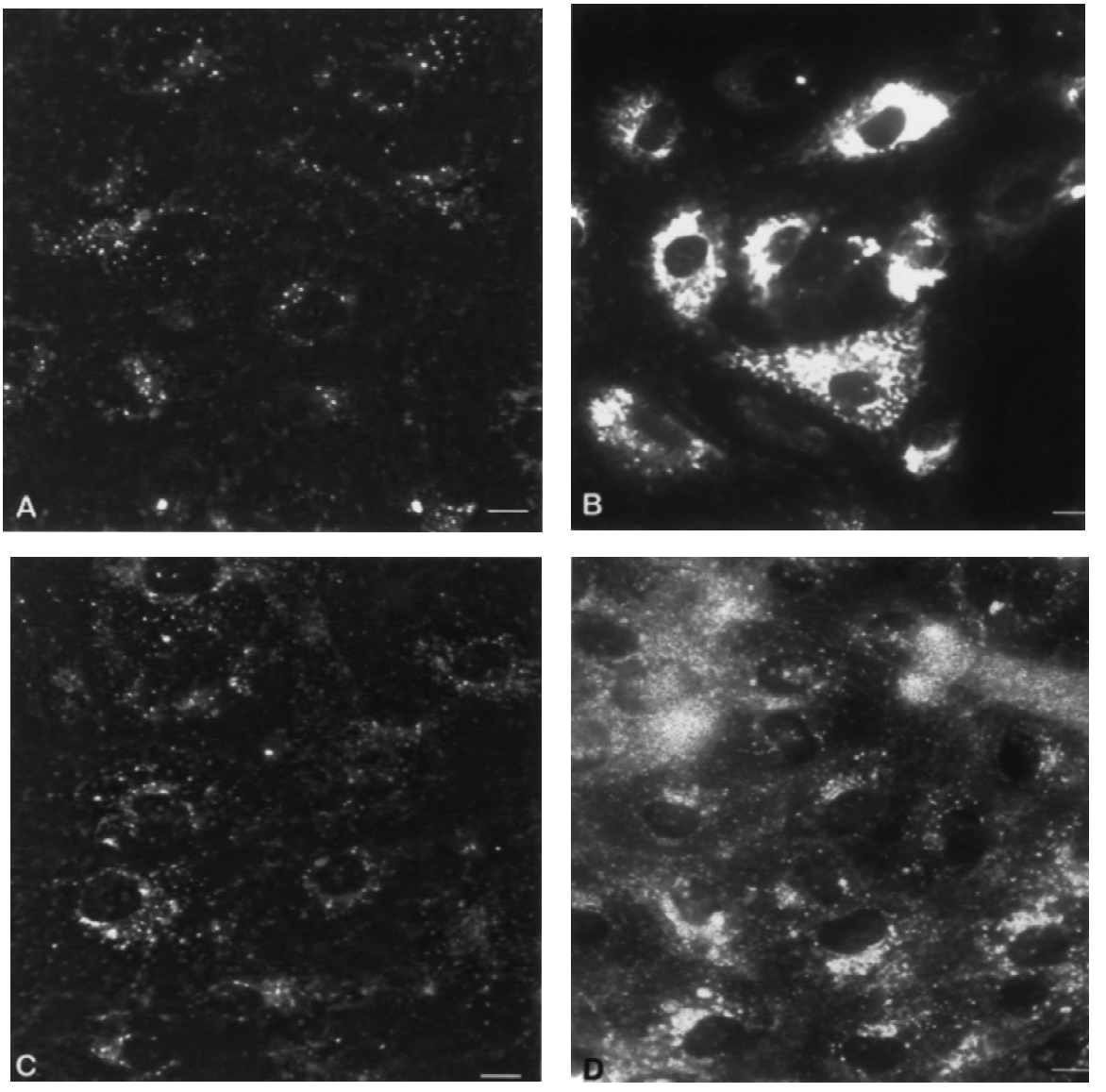

Fig. 11. Accumulation of excess styryl dye in endothelial cells induced by N-ethylmaleimide (NEM) and *botulinum* toxins A and B. (*A*) Control BPMVEC labeled with 5 μg/ml RH 414 in HBSS plus 10 mg/ml BSA for 5 min at 37°C. (*B*) BPMVEC incubated in 1 mM NEM for 5 min at 37°C, washed, and labeled as in (*A*). NEM caused endothelial cells to accumulate more particulate inclusions of dye resulting in greater brightness. (*C*) BPMVEC incubated for 6 hr in 100 ng/ml *Botulinum* toxin type A prior to labeling as in *A.* (*D*) BPMVEC incubated for 6 h in 1 ng/ml *Botulinum* toxin type B prior to labeling as in A. Scale bars 10 μm.

membrane curvature regulated and guided by specific set of signaling molecules. The present results show the unequivocal plasmalemma origin of cytosolic vesicles in endothelial cells.

An unexpected observation was that at least 50% of membrane vesiculation in endothelial cells is sustained by extracellular albumin over the physiological range (concentrations of 30–70 mg/ml). Albumin is known to stimulate endocytosis and transcytosis in mouse pulmonary and myocardial endothelium (Ghitescu et al., 1986; Milici et al., 1987). Thus, vesicle formation by albumin and its transcytosis may provide a mechanism for the continual equilibration of albumin between plasma and extracellular fluid. The present study indicates that the number of clathrin-coated vesicles as detected by dil-LDL uptake is ~1% of the total number of vesicles; therefore, formation of vesicles by scission of uncoated pits or caveolae (Schnitzer et al., 1994) may be the dominant mode of vesicle traffic in endothelial cells.

We found that albumin stimulated endocytosis by a mechanism distinct from the actual budding mechanism. PI 3-kinase inhibitors blocked endocytosis independently

of extracellular albumin, whereas tyrosine kinase inhibitors prevented only the albumin-dependent component of endocytosis. PI 3-kinase is believed to induce endocytosis secondary to activating membrane fusion between endosomes and intracellular compartments (Rameh, Chen & Cantley, 1995; Carpenter & Cantley, 1996). Since the endocytosis blocked by wortmanni was not accompanied by accumulation of labeled intracellular membrane, the present findings suggest that PI 3-kinase has an important role in membrane budding and fission in endothelial cells whereas tyrosine kinases regulate the albumin-activated vesicle formation.

The effect of tyrosine kinase inhibitors described in the present study implicates a role for tyrosine phosphorylation in signalling the albumin-mediated induction of endocytosis. Albumin binding to endothelial plasmalemma albumin-binding protein gp60 stimulates tyrosine phosphorylation of gp60, which may in turn activate endocytosis by tyrosine phosphorylation of caveolin-1 (Tiruppathi et al., 1997). Further studies will be needed to determine the signals by which the albumin receptor, gp60, is coupled to vesicle formation and the role of tyrosine kinases, plasmalemma-cytokeleton anchors such as ARF-6 (D'Souzza-Schorey et al., 1995), and GTPases such as rab17 (Zacchi et al., 1998) in the activation of endocytosis.

Rates of Endocytosis and Exocytosis in Endothelial Cells

Our data indicate that plasmalemma-derived vesicles undergo several possible fates including both rapid and slow exocytosis. We did not detect any change in the size and brightness of vesicles that disappeared when labeled cells were observed on the microscope stage. The vesicles did not undergo fusion events with intracellular processing compartments as would be expected for receptor recycling prior to release of dye to the external medium. Vesicles instead underwent exocytosis in a manner consistent with rapid transcytosis (Ghitescu et al., 1986; Milici et al., 1987). We observed that endothelial cells began to release dye as soon as they were labeled. The effect of exocytosis poisons NEM and *botulinum* toxin types A and B in inducing the accumulation of an extraordinary number of vesicles enabled estimation of this rapid rate. We represent the particulate dye distribution in endothelial cells as a pseudo-steady state between endocytosis and exocytosis with the Poisson jump process $X_1 \rightarrow X_2 \rightarrow X_3$ (Parzen, 1967), where state X_1 denotes a plasmalemma unit available for endocytosis, X_2 is a plasmalemma-derived vesicle, X_3 is membrane returned to the plasmalemma by fusion, and v_1 and v_2 are transition rate constants for endocytosis and exocytosis. During dye incubation, new vesicles enter state X_2 at the rate $1 - e_1^{-vt}$, and the endocytosis kinetics (Fig. 4*B*) are well-fitted by this expression with $v_1 = 0.131 \pm 0.053$ min^{-1} ($R^2 = 0.992$). Dye is lost from cells at the rate e_2^{-vt} (our data reveal several distinct loss processes that dominate at different time scales). This model predicts that the ratio of vesicle number in poisoned cells to that of normal cells is given by

$$\frac{v_1 + v_2}{v_1} \cdot \frac{1 - e_1^{-v\,t}}{1 - e_{1\ 2}^{-(v+v)t}}$$

where t is labeling duration. Since exocytosis poisons caused vesicle number to increase 3-fold over unpoisoned cells for the 5-min labeling period, the calculated rate constant v_2 for fast exocytosis is 0.26 min^{-1}. This time is consistent with release of Lucifer Yellow by cultured brain endothelial cells (Guillot, Audus & Raub, 1990).

Transcytosis in endothelial cells occurs over a wide time course that may depend on origin of cells, tracer, and method of determination. For example, colloidal gold-albumin conjugates perfused through mouse vasculature begin to appear in pericapillary spaces of lung and myocardium within 15 sec as determined by electron microscopy of fixed tissue (Ghitescu et al., 1986; Milici et al., 1987). Release of colloidal gold by pulmonary vascular endothelial as determined by absorbance occurs at a rate of 0.05% hr^{-1} (Schnitzer & Bravo, 1993) and temperature-dependent flux of ^{14}C-sucrose through cultured cerebrovascular endothelial cell monolayers occurs at 0.02 % hr^{-1} (Descamps et al., 1996). Although we did not study transcytosis, these values are similar to the >95% removal of styryl pyridinium dyes from cultured endothelial cells occurring over 24 hr as observed by us. However, we also observed the rapid disappearance of vesicles within an hour, which is similar to the 15 min kinetics of fluorescent albumin release by endothelial cells from rat epididymal fat (Williams, Greener & Solenski, 1984). The complex nature of the kinetics of plasmalemma-derived vesicles in endothelial cells observed in the present study suggests the intracellular sorting of vesicles in endothelial cells.

In summary, we have identified features of membrane dynamics in endothelial cells important in vesicle trafficking. The results support the hypothesis that endocytosis involves the formation of discrete vesicles derived from plasmalemma, followed by their translocation and then exocytosis. Data obtained using inhibitors suggest that the activation of endocytosis induced by albumin occurs via a tyrosine kinase pathway. Endocytosis and exocytosis in endothelial cells are distinct and separately regulated processes which involve PI 3-kinase and the SNARE machinery, respectively.

We thank Asma Naqvi for expert assistance in the culture and maintenance of endothelial cells. Supported by National Institutes of Health, grants T32 HL07829 and HL27016, HL46350 and HL45638.

References

Aikens, R.S., Agard, D.A., Sedat, J.W. 1989. Solid-state imagers for microscopy. *Meth. Cell Biol.* **29:**291–313

Anderson, R.G.W. 1993. Caveolae: Where incoming and outgoing messengers meet. *Proc. Natl. Acad. Sci. USA* **90:**10909–10913

Antohe, F., Serban, G., Radulescu, L., Simionescu, M. 1997. Transcytosis of albumin in endothelial cells is brefeldin A-independent. *Endothelium* **5:**125–136

Betz, W.J., Bewick, G.S., Ridge, R.M.A.P. 1992. Intracellular movements of fluorescently labeled synaptic vesicles in frog motor nerve terminals during nerve stimulation. *Neuron* **9:**805–813

Block, M.R., Glick, B.S., Wilcox, C.A., Wieland, F.T., Rothman, J.E. 1988. Identification of an N-ethylmaleimide-sensitive protein catalyzing vesicular transport. *Proc. Natl. Acad. Sci. USA* **85:**7852–7856

Carpenter, C.L., Cantley, L.C. 1996. Phosphoinositide kinases. *Curr. Opin. Cell Biol.* **8:**153–158

Clough, G. 1983. The dependence of vesicular transport on various physiological parameters. *Prog. Applied Microcirc.* **1:**35–50

Del Vecchio, P.J., Siflinger-Birnboim, A., Belloni, P.N., Holleran, L.A., Lum, H., Malik, A.B. 1992. Culture and characterization of pulmonary microvascular endothelial cells. *In Vitro Cell Dev. Biol.* **28A:**711–715

Descamps, L., Dehouck, M.-P., Torpier, G., Cecchelli, R. 1996. Receptor-mediated transcytosis of transferrin through blood-brain barrier endothelial cells. *Am. J. Physiol.* **270:**H1149–H1158

Döbereiner, H.G., Käs, J., Noppl, D., Sprenger, I., Sackmann, E. 1993. Budding and fission of vesicles. *Biophysical J.* **65:**1396–1403

Dunn, K.W., McGraw, T.E., Maxfield, F.R. 1989. Iterative fractionation of recycling receptors from lysosomally destined ligands in an early sorting endosome. *J. Cell Biol.* **109:**3303–3314

Dvorak, A.M., Kohn, S., Morgan, E.S., Fox, P., Nagy, J.A., Dvorak, H.F. 1996. The vesiculo-vacuolar organelle (VVO): a distinct endothelial cell structure that provides a transcellular pathway for macromolecular extravasation. *J. Leukocyte Biol.* **59:**100–115

Etaiw, S.H., Samy, S.S., Fayed, T.A. 1993. Absorption and emission characteristics of 2-styryl-1,6-dimethyl pyridinium iodide. *Can. J. Applied Spectroscopy* **38:**27–32

Folkman, J., Haudenschild, C.C., Zetter, B.R. 1979. Long-term culture of endothelial cells. *Proc. Natl. Acad. Sci. USA* **76:**5217–5221

Frøkjær-Jensen, J. 1991. The endothelial vesicle system in cryofixed frog mesenteric capillaries analyzed by ultrathin serial sectioning. *J. Electron Microscopy Tech.* **19:**291–304

Fujimoto, T., Miyawaki, A., K. Mikoshiba. 1995. Inositol 1,4,5-triphosphate receptor-like protein in plasmalemma caveolae linked to actin filaments. *J. Cell Sci.* **108:**7–15

Garcia, J.G.N., Siflinger-Birnboim, A., Bizios, R., Del Vecchio, P.J., Fenton, J.W. II, Malik, A.B. 1986. Thrombin-induced increase in albumin permeability across the endothelium. *J. Cell Physiol.* **128:**96–104

Ghitescu, L., Fixman, A., Simionescu, M., Simionescu, N. 1986. Specific binding sites for albumin restricted to plasmalemma vesicles of continuous capillary endothelium: Receptor-mediated transcytosis. *J. Cell Biol.* **102:**1304–1311

Guillot, F.L., Audus, K.L., Raub, T.J. 1990. Fluid-phase endocytosis by primary cultures of bovine brain microvessel endothelial cell monolayers. *Microvasc. Res.* **39:**1–14

Hammersen, F., Hammersen, E., Osterkamp-Baust, U. 1983. Structure and function of the endothelial cell. An introduction. *Prog. Applied Microcirc.* **1:**1–16

Inoué, S. 1986. Video Microscopy. Plenum, NY

Jeffries, W.A., Brandon, M.R., Hunt, S.V., Williams, A.F., Gatter, K.C., Mason, D.Y. 1984. Transferrin receptor on endothelium of brain capillaries. *Nature* **312:**162–163

Joly, M., Kazlauskas, A., Corvera, S. 1995. Phosphatidyl inositol 3-kinase activity is required at a post endocytic step in platelet-derived growth factor receptor trafficking. *J. Biol. Chem.* **270:**13225–13230

King, G.L., Johnson, S.M. 1981. Receptor-mediated transport of insulin across endothelial cells. *Science* **227:**1583–1586

Klausner, R.D., Donaldson, J.G., Lippincott-Schwartz, J. 1992. Brefeldin A: Insights into the control of membrane traffic and organelle structure. *J. Cell Biol.* **116:**1071–1080

Kozaki, S. 1979. Interaction of Botulinum type A, B, and E derivative toxins with synaptosomes of rat brain. *Naunyn-Schmiedebergs Arch. Pharmacol.* **308:**67–70

Liu, P., Ying, Y., Ko, Y.G., Anderson, R.G. 1996. Localization of platelet-derived growth factor-stimulated phosphorylation cascade to caveolae. *J. Biol. Chem.* **271:**10299–10303

Lum, H., Malik, A.B. 1994. Regulation of vascular endothelial barrier function. *Am. J. Physiol.* **267:**L223–241

Melikyan, G.B., White, J.M., Cohen, F.S. 1995. GPI-anchored influenza hemagglutinin induces hemifusion to both red blood cell and planar bilayer membranes. *J. Cell Biol.* **131:**679–691

Michel, C.C. 1992. The transport of albumin: A critique of the vesicular system in transendothelial transport. *Am. Rev. Resp. Dis.* **146:**S32–S36

Milici, A.J., Watrous, N.E., Stukenbrok, H., Palade, G.E. 1987. Transcytosis of albumin in capillary endothelial cells. *J. Cell Biol.* **105:**2603–2612

Murthy, V., Stevens, C.F. 1998. Synaptic vesicles retain their identity through the endocytic cycle. *Nature* **392:**497–501

Niles, W.D., Cohen, F.S. 1987. Video fluorescence microscopy studies of phospholipid vesicle fusion with a planar phospholipid membrane. Nature of membrane-membrane interactions and detection of release of contents. *J. Gen. Physiol.* **90:**703–735

Niles, W.D., Li, Q., Cohen, F.S. 1992. Computer detection of the rapid diffusion of fluorescent membrane fusion markers in images observed with video microscopy. *Biophysical J.* **63:**710–722

Palade, G.E. 1953. Fine structure of blood vessels. *J. Applied Physiol.* **24:**1423–1437

Parda, S.K., Mishra, B.K. 1996. Adsorption of styryl pyridinium dyes on silica gel. *J. Coll. Interface Sci.* **182:**473–477

Parton, R.G. 1996. Caveolae and caveolins. *Curr. Opin. Cell Biol.* **8:**542–548

Parzen, E. 1967. Stochastic Processes. Holden-Day, San Francisco, CA

Pellegrini, L.L., O'Connor, V., Lottspeich, F., Betz, H. 1995. Clostridial neurotoxins compromise the stability of a low energy SNARE complex mediating NSF activation of synaptic vesicle fusion. *EMBO J.* **14:**4705–4713

Pitas, R.E., Boyles, J., Mahley, R.W., Bissell, D.M. 1985. Uptake of chemically modified low density lipoproteins in vivo is mediated by specific endothelial cells. *J. Cell Biol.* **100:**103–117

Predescu, D., Horvat, R., Predescu, S., Palade, G.E. 1994. Transcytosis in the continuous endothelium of the myocardial microvasculature is inhibited by N-ethylmaleimide. *Proc. Natl. Acad. Sci. USA* **91:**3014–3018

Predescu, D., Simionescu, M., Simionescu, N., Palade, G.E. 1988. Binding and transcytosis of glycoalbumin by the microvascular endothelium of the murine myocardium: Evidence that glycoalbumin behaves as a bifunctional ligand. *J. Cell Biol.* **107:**1729–1738

Rameh, L.E., Chen, C.-W., Cantley, L.C. 1995. Phosphatidylinositol (3,4,5) P3 interacts with SH2 domains and modulates PI 3-kinase association with tyrosine-phosphorylated proteins. *Cell* **83:**821–830

Renkin, E.M. 1985. Capillary transport of molecules: Pores and other endothelial pathways. *J. Applied Physiol.* **58:**315–325

Renkin, E.M. 1992. Cellular and intercellular transport pathways in exchange vessels. *Am. Rev. Resp. Dis.* **146:**S28–31

Rothman, J.E. 1994. Mechanisms of intracellular protein transport. *Nature* **372:**55–62

Russ, J.C. 1992. The Image Processing Handbook. First edition. The CRC Press, Boca Raton, FL

Schnitzer, J.E., Allard, J., Oh, P. 1995*a*. NEM inhibits transcytosis, endocytosis, and capillary permeability: implication of caveolae fusion in endothelia. *Am. J. Physiol.* **268:**H48–H55

Schnitzer, J.E., Bravo, J. 1993. High affinity binding, endocytosis, and degradation of conformationally modified albumins. Potential role of gp30 and gp18 as novel scavenger receptors. *J. Biol. Chem.* **268:**7562–7570

Schnitzer, J.E., Liu, J., Oh, P. 1995*b*. Endothelial caveolae have the molecular transport machinery for vesicle budding, docking, and fusion including VAMP, NSF, SNAP, annexins, and GTPases. *J. Biol. Chem.* **270:**14399–404

Schnitzer, J.E., Oh, P., McIntosh, D.P. 1996. Role of GTP hydrolysis in fission of caveolae directly from plasma membranes. *Science* **274:**239–242

Schnitzer, J.E., Siflinger-Birnboim, A., Del Vecchio, P.J., Malik, A.B. 1994. Segmental differentiation of permeability, protein glycosylation, and morphology of cultured bovine lung vascular endothelium. *Biochem. Biophys. Res. Comm.* **199:**11–19

Simionescu, M., Simionescu, N. 1985. Functions of the endothelial cell surface. *Ann. Rev. Physiol.* **48:**279–293

D'Souzza-Schorey, C., Li, G., Colombo, M.I., Stahl, P.D. 1995. A regulatory role for ARF6 in receptor-mediated endocytosis. *Science* **267:**1175–1178

Tiruppathi, C., Song, W., Bergenfeldt, M., Sass, P., Malik, A.B. 1997. Gp60 activation mediates albumin transcytosis in endothelial cells by tyrosine-kinase-dependent pathway. *J. Biol. Chem.* **272:**25968–25975

Turro, N.J. 1978. Modern Molecular Photochemistry. Benjamin/Cummings Publishing, Menlo Park, CA

Williams, S.K., Greener, D.A., Solenski, N.J. 1984. Endocytosis and exocytosis of protein in capillary endothelium. *J. Cellular Physiol.* **120:**157–162

Zacchi, P., Stenmark, H., Parton, R.G., Orioli, D., Lim, F., Giner, A., Mellman, I., Zerial, M., Murphy, C. 1998. Rab 17 regulates membrane trafficking through apical recycling endosomes in polarized epithelial cells. *J. Cell Biol.* **140:**1039–1053